

The novel endoplasmic reticulum (ER)-targeted protein HAP induces cell apoptosis by the depletion of the ER Ca^{2+} stores

Xiaoling Qu, Yipeng Qi*, Ping Lan, Qilan Li

Institute of Virology, College of Life Sciences, Wuhan University, Wuhan 430072, PR China

Received 10 June 2002; revised 26 August 2002; accepted 29 August 2002

First published online 12 September 2002

Edited by Vladimir Skulachev

Abstract HAP, a novel human apoptosis-inducing protein, was identified to localize exclusively to the endoplasmic reticulum (ER) in our previous work. In the present work, we reported that ectopic overexpression of HAP proteins caused the rapid and sustained elevation of the intracellular cytosolic Ca^{2+} , which originated from the reversible ER Ca^{2+} stores release and the extracellular Ca^{2+} influx. The HeLa cells apoptosis induced by HAP proteins was not prevented by establishing the clamped cytosolic Ca^{2+} condition, or by buffering of the extracellular Ca^{2+} with EGTA, suggesting that the depletion of ER Ca^{2+} stores rather than the elevation of cytosolic Ca^{2+} or the extracellular Ca^{2+} entry contributed to HAP-induced HeLa cells apoptosis. Caspase-3 was also activated in the process of HAP-triggered apoptotic cell death.

© 2002 Published by Elsevier Science B.V. on behalf of the Federation of European Biochemical Societies.

Key words: Apoptosis-inducing protein HAP; Endoplasmic reticulum; Depletion of ER Ca^{2+} stores; Caspase-3 activation

1. Introduction

Apoptosis, an evolutionarily conserved programmed cell death process, is essential for the development, the maintenance of tissue homeostasis, and the elimination of excess or harmful cells in metazoan organisms [1]. A variety of stimuli, including cytokines, anti-cancer drugs, growth factor deprivation and so on, can cause a cell to undergo apoptosis characterized by a series of stereotypic morphological and biochemical features [2]. Up to now, many apoptosis-related genes have been identified and characterized. Li et al. [3] cloned a novel human apoptosis-inducing gene *ASY* which encodes an endoplasmic reticulum (ER)-targeting protein. In the previous work, we isolated another novel human apoptosis-inducing gene encoding the *ASY* interaction protein, designated as *hap* (homologue of *ASY* protein) [4,5]. As *ASY*, HAP protein

also exclusively localizes to the ER, and has no homology to other known apoptosis-related domains [6].

ER is well characterized as a mobilizable calcium store that sequesters excess cytosolic calcium and a reservoir for calcium signaling to maintain intracellular Ca^{2+} homeostasis [7]. A growing body of evidence suggested that changes in intracellular Ca^{2+} homeostasis play an important role in the modulation of apoptosis [8,9]. Various cell death stimuli including growth factor withdrawal [10], hormonal stimulation [11], and drug treatment [9] are known to alter the concentration of Ca^{2+} in the cytosol and the storage of Ca^{2+} in the intracellular organelles, which plays some roles in the cell death pathway. Agents that directly mobilize Ca^{2+} , e.g. Ca^{2+} ionophores or the sarcoplasmic/endoplasmic reticulum Ca^{2+} -ATPase inhibitor thapsigargin (TG), have been shown to trigger apoptosis in diverse cell types [12]. Furthermore, recent evidence showed that BCL-2 protein might suppress apoptosis via a mechanism that decreases the Ca^{2+} stores within the ER [13], or the mechanism that controls the apoptotic cross-talk between the ER and the mitochondria [14]. Based on such background information, we therefore speculate that the specific ER-targeted apoptosis-inducing protein HAP might trigger apoptosis by interfering with certain ER functions and the intracellular Ca^{2+} homeostasis, which prompted us to investigate the significance of Ca^{2+} in the signal transduction pathway of HAP-induced apoptosis process.

In the present study, we demonstrated that HAP overexpression induced the changes in cytosolic Ca^{2+} as well as ER Ca^{2+} content. The data further revealed that the depletion of ER Ca^{2+} stores rather than the elevation of intracellular Ca^{2+} or the extracellular Ca^{2+} influx played the pivotal role in HAP-induced HeLa cells apoptosis.

2. Materials and methods

2.1. Materials

TG, BAPTA/AM (1,2-bis(2-aminophenoxy)ethane-*N,N,N',N'*-tetraacetic acid tetrakis(acetoxymethyl)ester), EGTA (ethylene glycol-bis(2-aminoethyl)-*N,N,N',N'*-tetraacetic acid), Hoechst 33342, propidium iodide (PI), and Triton X-100 were purchased from Sigma. The fluorescent Ca^{2+} indicator Fura-2 acetoxymethyl ester (Fura-2/AM) was purchased from Molecular Probes, Eugene, OR, USA. The CaspACE[®] Assay System and the Lipofectamine[™] 2000 Reagent were obtained from Gibco/BRL. The mouse anti-poly(ADP-ribose) polymerase (PARP) monoclonal antibody (clone CII-10) was purchased from Roche. RNase A and proteinase K were the products of Promega. Other chemicals were analytic grade.

2.2. Construction of plasmids

The coding region sequence (*EcoRV* ~ *NotI* restriction fragment) of

*Corresponding author. Fax: (86)-27-87661831.

E-mail address: qiyipeng@whu.edu.cn (Y. Qi).

Abbreviations: ER, endoplasmic reticulum; HAP, homologue of *ASY* protein; TG, thapsigargin; BAPTA/AM, 1,2-bis(2-aminophenoxy)ethane-*N,N,N',N'*-tetraacetic acid tetrakis(acetoxymethyl)ester; EGTA, ethylene glycol-bis(2-aminoethyl)-*N,N,N',N'*-tetraacetic acid; PI, propidium iodide; Fura-2/AM, Fura-2 acetoxymethyl ester; EGFP, enhanced green fluorescence protein; PBS, phosphate-buffered saline; TBS, Tris-buffered saline; PARP, poly(ADP-ribose) polymerase; FCM, flow cytometry

hap gene cleaved out from the pSK*hap* plasmid (stored by this laboratory) was ligated into the compatible restriction sites in the multiple cloning site of pIRES-EGFP plasmid to get the recombinant plasmid pIRES-HAP-EGFP. This vector permits both the *hap* gene with transcription driven by the cephalomyocarditis virus promoter and the SV40 promoter-driven enhanced green fluorescence protein (EGFP) gene to be translated from a single bicistronic mRNA, providing a convenient way for efficiently sorting HAP-overexpressing cells on the basis of their EGFP fluorescence. The empty vector expressing EGFP alone was used for control purpose. The correct cloning was confirmed by corresponding restriction cleavage and sequencing.

2.3. Cell culture and transfections

The HeLa cells were maintained in RPMI 1640 medium (Gibco/BRL) supplemented with 10% heat-inactivated fetal calf serum, 4 mM L-glutamine, 100 U/ml penicillin, and 100 µg/ml streptomycin in a humidified atmosphere of 5% CO₂ and 95% air at 37°C. Plasmids were introduced into cells by using the LipofectamineTM 2000 Reagent (Gibco/BRL) following manufacturer's instructions. Transient expression of HAP-EGFP or EGFP proteins was assayed 10–72 h post-transfection by confocal fluorescence microscopy analysis or by flow cytometric analysis.

2.4. Transmission electron microscopic analysis

At 24 h after transfection, the HAP-overexpressing (indicated as EGFP-positive) and untransfected (indicated as EGFP-negative) cells which were identified by flow sorting were harvested, washed with cacodylate buffer (pH 7.4), and fixed for 2 h in 2.5% glutaraldehyde in 0.1 M cacodylate buffer (pH 7.4), respectively. After washing in buffer, the cells were post-fixed in 2% osmium tetroxide plus 1% potassium ferricyanide in cacodylate buffer, dehydrated through a graded alcohol series, embedded in Epon, thin-sectioned, stained with uranyl acetate and lead citrate, and observed by a Hitachi H-800 transmission electron microscope.

2.5. Flow cytometric analysis

Twenty-four hours after transfection, cells (including those that had detached and those remaining adherent) were collectively harvested in phosphate-buffered saline (PBS) containing 0.1% EDTA, washed twice with PBS, resuspended in PBS containing 3 mM sodium citrate, 0.1% Triton X-100, 20 µg/ml RNase A, and 50 µg/ml PI, and incubated for 30 min at 37°C in the dark. The cells transfected with pIRES-HAP-EGFP or pIRES-EGFP expression vectors were analyzed for EGFP and PI fluorescence on a FACScan flow cytometer (Becton Dickinson). The EGFP and PI fluorescence were measured using a 509 nm and a 620 nm band pass filter, respectively. Data analysis was performed using the CellQuest software program.

2.6. DNA fragmentation analysis

Cells (2×10^5 per sample) were harvested and washed with PBS, incubated for 1 h at 50°C in 0.5 ml of lysis buffer (0.1% Triton X-100, 50 mM Tris-HCl, pH 8.0, 10 mM EDTA-Na₂, and 200 mM NaCl) supplemented with proteinase K (5 mg/ml). DNase-free RNase A was added (20 µg/ml of lysate) and incubated at 56°C for 2 h with gentle shaking. After extractions with phenol twice and once with phenol/chloroform/isoamylalcohol (25:24:1), the DNA was precipitated with one-tenth volume of 5 M ammonium acetate (pH 5.2) and two volumes of absolute ethanol at -20°C for overnight, washed with ice-cold 70% ethanol, air-dried, resolved in 50 µl TBE buffer (10 mM Tris, 1 mM EDTA-Na₂, pH 8.0). DNA was separated by electrophoresis on a 1.5% agarose gel and visualized by ethidium bromide staining (0.5 µg/ml) under ultra-violet light.

2.7. Hoechst 33342 staining

Cells seeded in chamber slides were washed twice with PBS, fixed in 4% paraformaldehyde for 20 min, washed again and stained with Hoechst 33342 (10 µg/ml) at 37°C for 20 min in the dark. After another wash with PBS, cells were viewed for the EGFP or Hoechst 33342 fluorescence under a fluorescence microscope (Olympus). Hoechst 33342 fluorescence was detected with the XF 67 filter (excitation = 340 nm, emission = 470 nm).

2.8. Measurement of $[Ca^{2+}]_i$

Cells (2×10^4 /dish) plated on coverslips coated with poly-L-lysine were transfected with pIRES-EGFP or pIRES-HAP-EGFP plasmids

or left untransfected. According to the preliminary study which demonstrated that the earliest time for green cells appearance was at 12 h post-transfection, the cells were incubated at 37°C for 45 min with Fura-2/AM (5 µM) in Krebs-Ringer buffer (140 mM NaCl, 2.8 mM KCl, 2 mM MgCl₂, 2 mM CaCl₂, 20 mM HEPES, 1 mg/ml glucose, 1 mg/ml, pH 7.4) at 10 h after transfection. Coverslips with cells were washed with this buffer and mounted in a 35 mm holder maintained at 30°C. Based on the time-lapse observation, as soon as the cells displayed green fluorescence, the changes of Fura-2 fluorescence were monitored in certain single cells by dual excitation imaging using an Attofluor Digital Fluorescence Microscopy System (Atto Instruments Inc.). $[Ca^{2+}]_i$ was calculated from the ratio of the fluorescence intensity ($R = F_{340}/F_{380}$) by using the formula described by Grynkiewicz et al. [15]: $[Ca^{2+}]_i = K_d[(R - R_{min})/(R_{max} - R)](F_{min}/F_{max})$, where R_{max} and R_{min} are the fluorescence ratios after treatment of cells with 0.1% (V/V) aqueous Triton X-100 and 3 mM EGTA, respectively, F_{max} and F_{min} are values of F_{380} after treatment with Triton X-100 and EGTA, respectively, and $K_d = 244$ nM.

2.9. Caspase-3 activity assay

Caspase-3 enzymatic activity was determined by monitoring the cleavage of the specific synthetic fluorogenic substrate Ac-DEVD-AMC by using the CaspACETM Assay System. For pIRES-HAP-EGFP- or pIRES-EGFP-transfected cells, at various time points (24, 48, and 60 h) post-transfection, cells were respectively harvested and washed briefly with cold PBS, lysed for 10 min at 4°C in lysis buffer (50 mM HEPES-KOH, pH 7.4, 1 mM EDTA buffer containing 75 mM NaCl, 0.1% Triton X-100, 1 mM dithiothreitol, 1 mM phenylmethylsulfonyl fluoride, 10 µg/ml pepstatin A, and 100 KIU/ml aprotinin), and spun at $10000 \times g$ for 20 min at 4°C, then the supernatants (cell lysates) were recovered separately. The protein content of each sample was determined by the Bio-Rad protein assay using bovine serum albumin as a standard. Enzymatic reactions (final volume, 250 µl) containing 50 µg of cell lysates and 200 µM of Ac-DEVD-AMC were performed in the reaction buffer (50 mM HEPES-KOH, pH 7.4, 75 mM NaCl, 1 mM EDTA, 1% CHAPS, 10% sucrose, and 2 mM dithiothreitol) for 1 h at 37°C. The caspase-3 activity was measured by using a flow cytometer at an excitation wavelength of 380 nm and an emission value of 440 nm.

2.10. PARP immunoblotting analysis

Cells were harvested at several time points post-transfection, washed twice with ice-cold PBS, and lysed with modified RIPA buffer (150 mM NaCl, 50 mM Tris-HCl, pH 8.0, 1 mM EGTA, 1% Triton X-100, 0.1% SDS, 1% sodium deoxycholate) in the presence of protease inhibitors (0.1 mM phenylmethylsulfonyl fluoride, 1.0 µM pepstatin, 1 mM benzamidine, 10 µM leupeptin, 1 µg/ml aprotinin). 100 µg of the whole cell lysate was subjected to SDS-polyacrylamide gel electrophoresis and subsequently transferred to polyvinylidene difluoride membranes. The membranes were blocked with Tris-buffered saline (TBS, 10 mM Tris-HCl, pH 8.0, 150 mM NaCl) containing 0.05% Tween 20 and 10% non-fat milk, and then probed with an anti-PARP monoclonal antibody (clone CII-10) diluted 1:5000 in 3% non-fat milk. The membranes were washed with TBS and then blotted with an anti-mouse secondary antibody conjugated to horseradish peroxidase (1:1000 dilution). The membranes were exposed using the enhanced chemiluminescence Western blotting analysis system (Amersham Pharmacia Biotech).

2.11. Statistical analysis

All values are expressed as the mean \pm S.E.M. of n observation ($n > 4$). In comparing two groups, statistical significance was determined by Student's *t*-test. A value of $P < 0.05$ was considered statistically significant.

3. Results

3.1. Ectopic expression of HAP proteins induced HeLa cells apoptosis

HAP overexpression-induced HeLa cells apoptosis was demonstrated based on the following features: ultrastructural morphological changes, hypodiploid DNA appearance, DNA fragmentation, chromatin condensation and nuclei break-

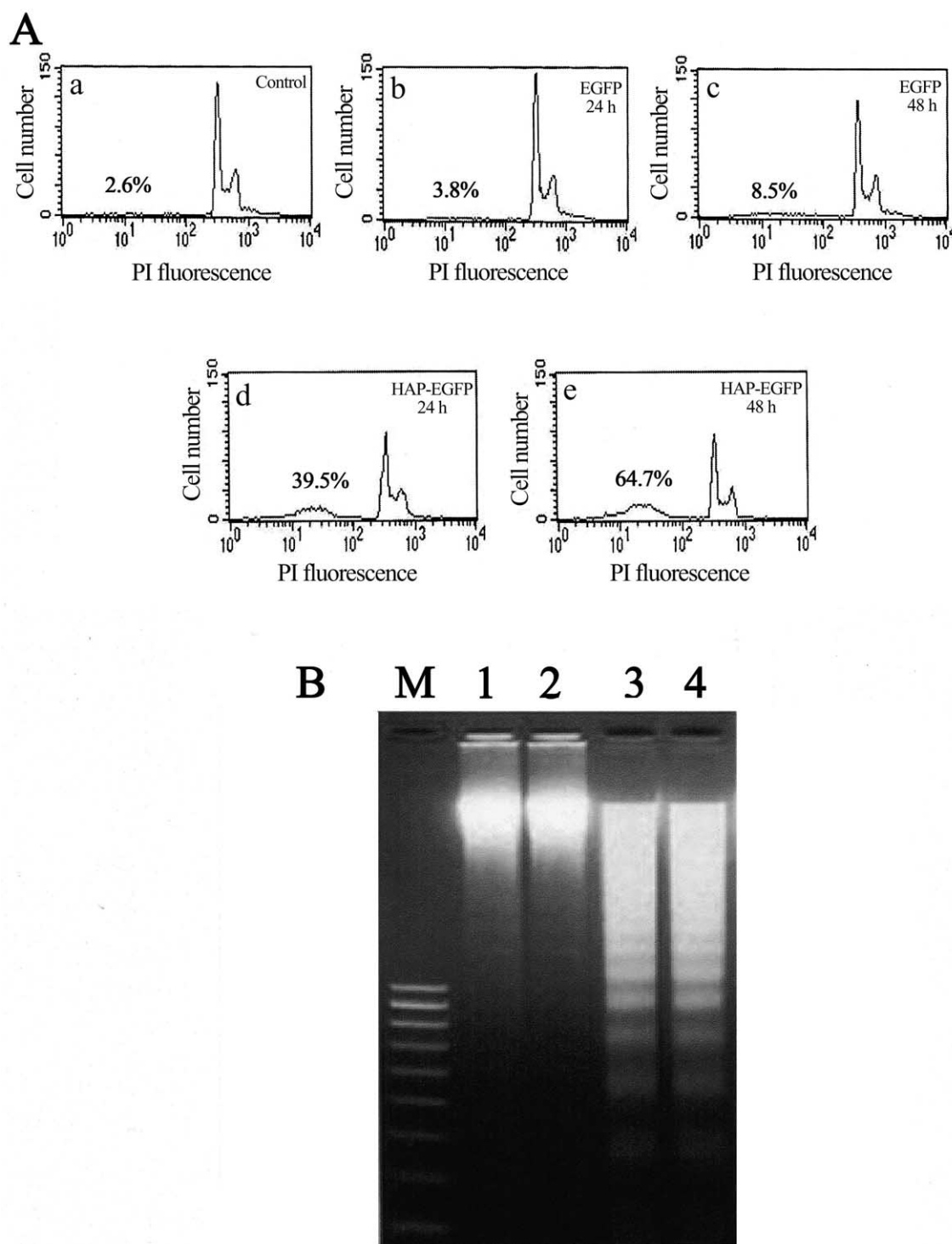


Fig. 1. Evidence for HAP overexpression-induced HeLa cells apoptosis. A: Flow cytometric analysis of the DNA content. DNA contents of the untransfected cells (a), the EGFP-expressing cells (b and c), and the HAP-expressing cells (d and e) were measured by FCM analysis, and the apoptotic cells were determined to be those that contained DNA below that of cells in the G1 phase. Results shown represent the mean of three independent experiments (mean \pm S.E.M.). B: DNA fragmentation analysis. Overexpression of HAP induced DNA fragmentation (lanes 3 and 4), but the characteristic DNA laddering pattern was absent in empty vector-transfected (lane 2) or untransfected (lane 1) HeLa cells.

down. The HAP-overexpressing HeLa cells revealed many ultrastructural features consistent with apoptosis: cytosolic density alteration, chromatin condensation and nuclear fragmentation, and the dilation of some organelles such as mitochondria and rough ER. Typically, the apoptotic body formation was also observed. The DNA content of HAP-

overexpressing HeLa cells was analyzed by flow cytometry (FCM). At 24 h after transfection, by gating EGFP-positive and EGFP-negative cells, 39.5% of cells expressing HAP-EGFP were determined to be apoptotic (Fig. 1A, d), compared with 3.8% (Fig. 1A, b) and 2.6% (Fig. 1A, a) apoptotic cells in the EGFP-overexpressing and untransfected cells pop-

ulation, respectively. Furthermore, the result showed that the apoptosis ratio in cells expressing HAP-EGFP increased to 64.7% at 48 h post-transfection (as shown in Fig. 1A, e), whereas the apoptosis ratio in cells expressing EGFP alone did not increase dramatically (8.5%) (Fig. 1A, c). Another common feature of cells undergoing apoptosis is the fragmentation of genomic DNA into laddering patterns of oligonucleosome-sized fragments. Fig. 1B is a representative agarose gel of extracted genomic DNA from HAP-transfected, EGFP-transfected or untransfected HeLa cells. In HAP-overexpressing cells, the DNA laddering pattern was clearly visible at 24 h

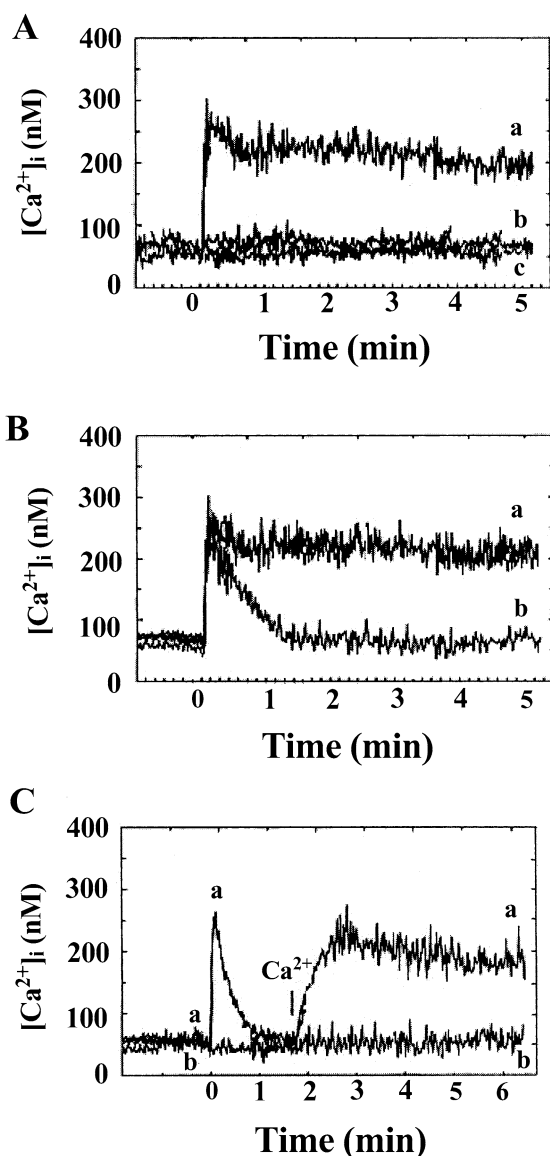


Fig. 2. The elevation of cytosolic Ca^{2+} induced by HAP proteins overexpression. A: HAP overexpression triggered the rapid and sustained increase of $[Ca^{2+}]_i$ (trace a), whereas no apparent $[Ca^{2+}]_i$ changes were measured in EGFP alone expressing (trace b) or untransfected (trace c) cells. B: The extracellular Ca^{2+} chelator EGTA blocked HAP overexpression-induced sustained Ca^{2+} rise (trace b), compared to no EGTA treatment (trace a). C: The dependence of HAP overexpression-induced Ca^{2+} influx on extracellular Ca^{2+} . Removing Ca^{2+} from the external medium blocked HAP-stimulated Ca^{2+} entry, while reintroduced extracellular Ca^{2+} restored Ca^{2+} entry (trace a). No change of $[Ca^{2+}]_i$ was detected in only EGFP-expressing cells upon the same treatment (trace b).

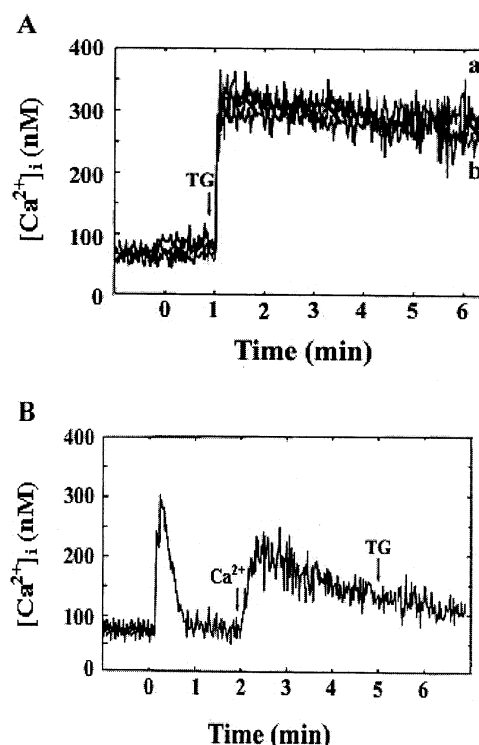


Fig. 3. The depletion of ER Ca^{2+} stores triggered by overexpression of HAP proteins. A: HeLa cells untransfected (trace b) or transfected with empty vector (trace a) showed a rapid response to TG stimulation, with a rise in cytosolic Ca^{2+} . B: HeLa cells with HAP overexpression lost response to TG administration even after reintroducing extracellular Ca^{2+} (2 mM).

post-transfection (lane 3), which continued to be observed at 48 h after transfection (lane 4). However, the untransfected cells (lane 1) and the EGFP-transfected cells (lane 2) showed no detectable DNA fragmentation. The morphological changes of the nuclei in individual transfected cells were also observed by the Hoechst 33342 staining. The results revealed that most cells overexpressing HAP proteins, which were identified by green fluorescence, exhibited condensed chromatin and fragmented nuclei, a characteristic feature of cells undergoing apoptosis, whereas the nuclei of only EGFP-overexpressing cells remained morphologically intact and with normal nuclear structure.

3.2. Overexpression of HAP proteins resulted in the elevation of cytosolic Ca^{2+}

Apoptosis-inducing protein HAP exclusively localizes to ER membrane, suggesting that it might exert some effects on the intracellular Ca^{2+} homeostasis to trigger the apoptosis. The intracellular Ca^{2+} state in HAP-overexpressing HeLa cells was therefore examined. As shown in Fig. 2A,B (trace a), in HeLa cells incubated in the bathing solution containing 2 mM extracellular calcium, HAP overexpression evoked Ca^{2+} signal with a characteristic biphasic: a rapid large initial rise in cytosolic Ca^{2+} as a result of the depletion of intracellular Ca^{2+} stores, with levels reaching ~280 nM, followed by a sustained phase of elevated $[Ca^{2+}]_i$, corresponding to the extracellular Ca^{2+} influx. This Ca^{2+} pool depletion-activated Ca^{2+} entry was confirmed by the fact that addition of EGTA to chelate extracellular Ca^{2+} diminished somewhat the size of

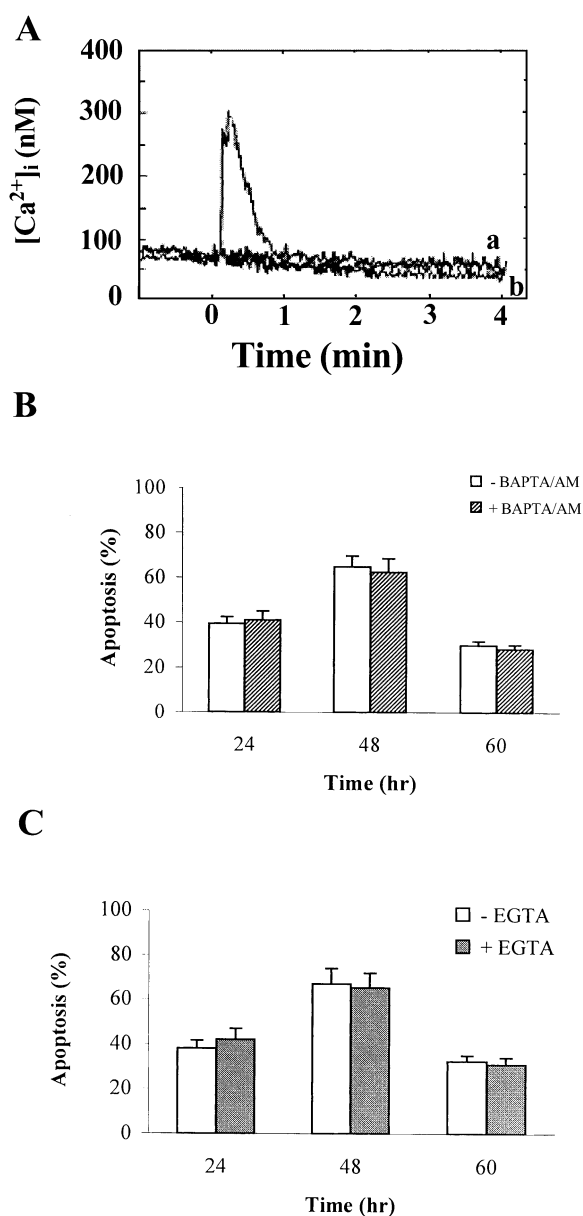


Fig. 4. The clamped cytosolic Ca^{2+} condition and the extracellular Ca^{2+} chelator EGTA failed to prevent HAP overexpression-induced HeLa cells apoptosis. A: Representative traces of HAP-overexpressing induced cytosolic Ca^{2+} increase in HeLa cells were plotted in untreated control (trace a) or in clamped cytosolic Ca^{2+} conditions (trace b). B: The clamped cytosolic Ca^{2+} condition did not affect HAP-induced apoptosis ratios at 24, 48, and 60 h after transfection. C: Pretreatment with EGTA did not prevent the HAP-induced apoptosis process at 24, 48, and 60 h post-transfection.

the initial increase of $[Ca^{2+}]_i$, and abolished the sequential sustained elevation (Fig. 2B, trace b). Decreasing the extracellular Ca^{2+} concentration to 1 μ M also suppressed Ca^{2+} entry while reintroducing extracellular Ca^{2+} (2 mM) restored cytosolic Ca^{2+} (as shown in Fig. 2C, trace a), whereas no $[Ca^{2+}]_i$ changes were detected in only EGFP-expressing cells when they underwent the same treatment (Fig. 2C, trace b). In addition, in untransfected (Fig. 2A, trace b) or EGFP alone expressing (Fig. 2A, trace c) HeLa cells, there were no changes of $[Ca^{2+}]_i$ during the same time periods, with basal $[Ca^{2+}]_i$ of ~ 80 –100 nM.

3.3. Overexpression of HAP proteins caused the depletion of ER Ca^{2+} stores

In view of the evidence that HAP protein exclusively localizes to ER, the possibility that HAP induced apoptosis by regulating Ca^{2+} fluxes through the ER membrane was investigated. Theoretically, if overexpressed HAP proteins led to ER Ca^{2+} release, then TG (a specific sarcoplasmic/endoplasmic reticulum Ca^{2+} -ATPase inhibitor which permits the direct assessment of the ER Ca^{2+} pool) administration should not cause additional Ca^{2+} release. In this study, HeLa cells left untransfected (Fig. 3A, trace b) or expressing EGFP alone (Fig. 3A, trace a) responded to the rapid release of Ca^{2+} from ER upon application of TG, with a rise in cytosolic Ca^{2+} . In contrast, a striking difference was observed with HAP-overexpressing HeLa cells, in which the cells lost responses to sequential TG stimulation even after prolonged incubation with 2 mM Ca^{2+} in the bathing solution (as shown in Fig. 3B), suggesting an empty ER Ca^{2+} pool as a result of HAP overexpression, and also indicating that HAP protein shared a common pool of releasable Ca^{2+} with TG, namely, the ER Ca^{2+} pool.

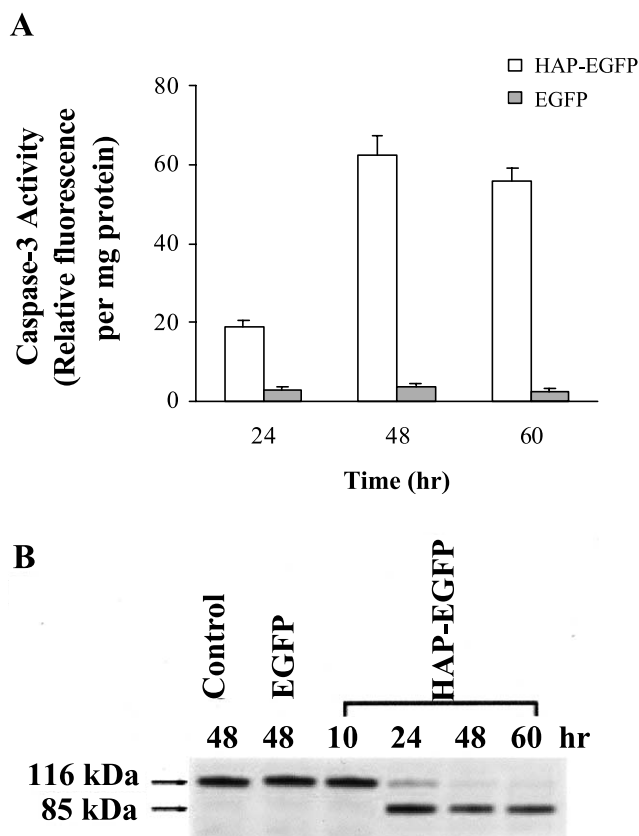


Fig. 5. Overexpression of HAP proteins induced the caspase-3 activation, as indicated by cleavage of the specific substrates. A: The cleavage of specific synthetic fluorogenic substrate by caspase-3 in HAP-overexpressing HeLa cells. The results are representative of three separate experiments. The data are mean \pm S.E.M. of three samples. B: The cell lysates were analyzed for the cleavage of the specific native substrate PARP by caspase-3. The intact PARP (116 kDa) was cleaved to an 85 kDa signature fragment in HAP-overexpressing HeLa cells.

3.4. The depletion of ER Ca^{2+} stores contributed to HAP-induced HeLa cells apoptosis

To determine which factor(s) might serve as the primary mediator for HAP-induced HeLa cells apoptosis, the effects of EGTA and the clamped cytosolic Ca^{2+} condition on HAP-induced apoptosis were studied. Having established certain conditions by culturing HeLa cells in RPMI 1640 medium with 110 μM extracellular Ca^{2+} and 7 μM BAPTA/AM, which sustained a cytosolic Ca^{2+} clamp yet did not deplete intracellular Ca^{2+} stores and induce apoptosis [16], the apoptosis in HAP-overexpressing HeLa cells was detected. As shown in Fig. 4A, in cells cultured in a certain clamped cytosolic Ca^{2+} condition, the HAP overexpression-induced rapid elevation of cytosolic Ca^{2+} was reduced dramatically (trace b, compared to trace a which served as the untreated control). Surprisingly, Hoechst 33342 staining of cellular nuclei did not reveal a visible difference compared to those of untreated cells. Furthermore, quantitative assays of apoptosis by using FCM analysis for the hypodiploid DNA gave nearly similar cell death indices irrespective of treatment with the clamped condition, at multiple time points after transfection (see Fig. 4B). In summary, buffering of cytosolic Ca^{2+} by establishing the clamped cytosolic Ca^{2+} condition did not appear to interfere with the HeLa cells apoptosis process induced by HAP overexpression. Similarly, buffering of the extracellular Ca^{2+} with EGTA (1 mM) to prevent the extracellular Ca^{2+} influx also failed to protect HeLa cells from HAP overexpression-induced nuclear fragmentation and chromatin condensation when compared with untreated control. In addition, the FCM analysis showed that HeLa cells apoptosis triggered by HAP overexpression proceeded along the time lapse even with EGTA treatment (as shown in Fig. 4C).

Taken together, these data suggested that the depletion of ER Ca^{2+} stores rather than the elevation of cytosolic Ca^{2+} or the extracellular Ca^{2+} entry contributed to HAP overexpression-induced HeLa cells apoptosis.

3.5. Overexpression of HAP proteins activated the caspase-3

In the present study, the activation of caspase-3 in HAP-overexpressing HeLa cells was evaluated by monitoring the cleavage of caspase-3-specific substrates. As shown in Fig. 5A, the resulting time-dependent apoptosis in HeLa cells triggered by HAP overexpression was accompanied by a corresponding time-dependent caspase-3 activation, as indicated by the cleavage of the specific synthetic fluorogenic substrate Ac-DEVD-AMC. In the cellular extracts of only EGFP-expressing cells, no caspase-3 activation was detected, as indicated by no cleavage of the specific substrate. Additionally, the activation of caspase-3 was further identified by the cleavage of its native substrate PARP, a commonly used measurement of caspase-3-like enzymatic activity. As shown in Fig. 5B, the intact PARP (116 kDa) was cleaved to an 85 kDa signature fragment in HAP-overexpressing HeLa cells, whereas cleavage of PARP was detected in EGFP-transfected or untransfected HeLa cells.

4. Discussion

In the present work, we demonstrated that overexpression of the novel ER-targeted protein HAP induced HeLa cells apoptosis, which exhibited the characteristic morphological and biochemical features of apoptosis, including ultrastructur-

al morphological changes, hypodiploid DNA occurrence, internucleosomal DNA fragmentation, chromatin condensation, nuclear fragmentation, and caspase-3 activation.

Although a growing body of evidence is emerging from different studies which suggest an active role for the ER in regulating apoptosis [17,18], mechanisms used within it in mediating apoptotic signals are not well understood. As the ER plays a central role in regulating intracellular Ca^{2+} signaling, and the high Ca^{2+} content of the ER lumen appears necessary for maintaining the structural and functional integrity of the ER as well as for a variety of other cellular functions, including cell division, cell cycle progression, and cell death [19], it is possible that ER Ca^{2+} pool depletion may contribute to the cellular and molecular mechanisms of ER stress-induced apoptosis. In this study, we revealed that overexpression of the novel ER-resident apoptosis-inducing protein HAP indeed led to the elevation of cytosolic Ca^{2+} , which might come from the rapid depletion of ER Ca^{2+} stores and the sequential sustained extracellular Ca^{2+} entry. The further data demonstrated that HAP overexpression-triggered HeLa cells apoptosis was not prevented by establishing the clamped cytosolic Ca^{2+} condition or chelating the extracellular Ca^{2+} with EGTA, suggesting that the depletion of ER Ca^{2+} pool rather than the elevation of cytosolic Ca^{2+} or the extracellular Ca^{2+} entry served as the critical mediator in the apoptotic signal transduction pathway of HAP protein. A certain concept that ER Ca^{2+} pool depletion mediates apoptosis is consistent with the findings of others. For example, Oyadomari et al. [20] stated that nitric oxide (NO) depleted ER Ca^{2+} stores, caused ER stress and led to apoptosis in pancreatic beta cells. Wertz et al. [16] reported that release of intracellular ER Ca^{2+} stores was sufficient to induce apoptosis of the LNCaP cell line. Additionally, ER Ca^{2+} pool depletion was not observed in cells transfected with BCL-2 [13,21], suggesting that part of BCL-2's anti-apoptotic mechanism involves the maintenance of the ER Ca^{2+} stores.

Although several studies, including the finding of our research work, suggested that depletion of ER Ca^{2+} stores mediates cell apoptosis, the precise mechanism remains unclear. Taken together all of the previous findings, two different apoptotic pathways have been suggested to mediate the signal transduction upon ER Ca^{2+} pool depletion-induced apoptosis. One is characterized by the activation of the ER-resident caspase-12, which is a mediator of ER-specific apoptosis and signals apoptotic pathway in a mitochondria-independent way [22]. Alternatively, given the central role of mitochondria in the commitment to apoptosis as well as the close physical interaction between the mitochondrial and ER network [23], it is possible that ER Ca^{2+} pool depletion triggers secondary changes in mitochondrial Ca^{2+} levels which contribute to cytochrome *c* release and cell death. In fact, a lot of recent studies have shown certain cross-talk existing between the ER and mitochondrial Ca^{2+} handling as well as the cell death signals. For instance, Nutt and coworkers [24,25] recently demonstrated that overexpression of BAX resulted in early release of the ER Ca^{2+} pool and subsequent Ca^{2+} accumulation in mitochondria. Inhibition of mitochondrial Ca^{2+} uptake attenuated BAX-induced cytochrome *c* release and DNA fragmentation, strongly suggesting that BAX-mediated alterations in ER and mitochondrial Ca^{2+} levels serve as important upstream signals for cytochrome *c* release and apoptosis. Furthermore, Oyadomari et al. [20] proposed a mechanism

whereby depletion of the ER Ca^{2+} pool induces apoptosis in Jurkat T cells through a pathway involving an increase in cytosolic Ca^{2+} levels, followed by mitochondrial Ca^{2+} overloading and the Ca^{2+} -dependent NO production, the reduction in mitochondrial membrane potential, the release of mitochondrial cytochrome *c*, and the activation of caspase-3, suggesting there are close contacts between the ER and mitochondrial apoptosis signaling pathway. Given that our study provided some of the first evidence that HAP protein can induce HeLa cells apoptosis mediated by intracellular ER Ca^{2+} pool depletion, and also can lead to some responses in mitochondria, e.g. mitochondrial transmembrane potential reduction and cytochrome *c* release from mitochondria (unpublished personal data) etc., it is therefore possible that ER and mitochondria act as the coordinated regulators in the HAP-induced apoptotic signal transduction pathway. The exact cellular and molecular mechanisms of the HAP-triggered apoptotic pathway are under investigation.

It is noteworthy that the activation of caspase-3 was also verified in our study by the specific cleavage of the synthetic substrate or the native substrate PARP in the HeLa cells with HAP overexpression (as shown in Fig. 5). Then, how HAP protein-induced ER stress transduces the apoptotic signals to the downstream effector caspase-3 activation? We speculate that there are several probable pathways. One possible route is through the well-described release of mitochondrial cytochrome *c*, formation of the apoptosome, and activation of caspase-9, which in turn processes and activates downstream caspases such as caspase-3 and -6. An alternative possibility is the direct activation of caspase-3 by the specific ER-resident caspase-12, which is activated during the ER stress-induced apoptosis process [22,26].

Exactly how overexpressing HAP proteins affect the intracellular Ca^{2+} homeostasis is presently unknown, even though several potential mechanisms can be proposed here. First, the ER-targeted HAP protein may oligomerize and create a non-selective or selective ion pore across the ER membrane and may therefore cause leakage of Ca^{2+} from the ER stores, which resembles as the ER-bound BAX protein [27]. Second, HAP protein may interact directly or indirectly with the sarcoplasmic/endoplasmic reticulum Ca^{2+} pump, or the Ca^{2+} release channels (i.e. the inositol 1,4,5-trisphosphate receptor or the ryanodine receptor), and thus may affect the overall Ca^{2+} transport across the ER membrane. Another intriguing possibility could be that HAP protein might affect the communication between ER and mitochondria in the movement of Ca^{2+} . Further studies to investigate the possible cross-talk between ER Ca^{2+} release and mitochondrial Ca^{2+} uptake, and to understand the effect(s) of HAP protein on the contacts between ER and mitochondria signals should provide new insights into the cellular and molecular mechanisms of Ca^{2+} signaling in the apoptosis process induced by the novel apoptosis-inducing protein HAP.

Acknowledgements: This present work is supported by the National Nature Science Foundation Grant (30170455) of PR China.

References

- [1] Jacobson, M.D., Weil, M. and Raff, M.C. (1997) *Cell* 88, 347–354.
- [2] Green, D.R. (1998) *Cell* 94, 695–698.
- [3] Li, Q., Qi, B., Oka, K., Shimakage, M., Yoshioka, N., Inoue, H., Hakura, A., Kodama, K., Stanbridge, E.J. and Yutsudo, M. (2001) *Oncogene* 20, 3929–3936.
- [4] Qi, B., Qi, Y.P., Yutsudo, M. and Liu, Q.Z. (2000) *Sci. China (Ser. C)* 43, 310–320.
- [5] Qu, X.L., Qi, Y.P. and Qi, B. (2002) *Arch. Biochem. Biophys.* 400, 233–244.
- [6] Qi, B., Qi, Y.P., Liu, Q.Z. and Qu, X.L. (2001) *Chin. Sci. Bull.* 46, 1409–1411.
- [7] Sambrook, J.F. (1990) *Cell* 61, 197–199.
- [8] Pinton, P., Ferrari, D., Rappizzi, E., Di Virgilio, F.D., Pozzan, T. and Rizzuto, R. (2001) *EMBO J.* 20, 2690–2701.
- [9] Tagliarino, C., Pink, J.J., Dubyak, G.R., Nieminen, A.L. and Boothman, D.A. (2001) *J. Biol. Chem.* 276, 19150–19159.
- [10] Jayadev, S., Barrett, J.C. and Murphy, E. (2000) *AJP-Cell Physiol.* 279, C1604–C1647.
- [11] Wang, L., Bhattacharjee, A., Zuo, Z., Hu, F., Honkanen, R.E., Berggren, P.O. and Li, M. (1999) *Endocrinology* 140, 1200–1204.
- [12] Nakamura, K., Bossy-Wetzel, E., Burns, K., Fadel, M.P., Lozyk, M., Goping, I.S., Opas, M., Bleackley, R.C., Green, D.R. and Michalak, M. (2000) *J. Cell Biol.* 150, 731–740.
- [13] Foyouzi-Youssefi, R., Arnaudeau, S., Borner, C., Kelley, W.L., Tschopp, J., Lew, D.P., Demareux, N. and Krause, K.H. (2000) *Proc. Natl. Acad. Sci. USA* 97, 5723–5728.
- [14] Hacki, J., Egger, L., Monney, L., Conus, S., Rosse, T., Fellay, I. and Borner, C. (2000) *Oncogene* 19, 2286–2295.
- [15] Gryniewicz, G., Poenie, M. and Tsien, R.Y. (1985) *J. Biol. Chem.* 260, 3440–3450.
- [16] Wertz, I.E. and Dixit, V.M. (2000) *J. Biol. Chem.* 275, 11470–11477.
- [17] Zuppin, A., Groenendyk, J., Cormack, L.A., Shore, G., Opas, M., Bleackley, R.C. and Michalak, M. (2002) *Biochemistry* 41, 2850–2858.
- [18] Ferri, K.F. and Kroemer, G. (2001) *Nat. Cell. Biol.* 3, E255–E263.
- [19] Berridge, M.J., Bootman, M.D. and Lipp, P. (1998) *Nature* 395, 645–648.
- [20] Oyadomari, S., Takeda, K., Takiguchi, M., Gotoh, T., Matsumoto, M., Wada, I., Akira, S., Araki, E. and Mori, M. (2001) *Proc. Natl. Acad. Sci. USA* 98, 10845–10850.
- [21] He, H., Lam, M., McCormick, T.S. and Distelhorst, C.W. (1997) *J. Cell Biol.* 138, 1219–1228.
- [22] Nakagawa, T., Zhu, H., Morishima, N., Li, E., Xu, J., Yankner, B.A. and Yuan, J. (2000) *Nature* 403, 98–103.
- [23] Rizzuto, R., Pinton, P., Carrington, W., Fay, F.S., Fogarty, K.E., Lifshitz, L.M., Tuft, R.A. and Pozzan, T. (1998) *Science* 280, 1763–1766.
- [24] Nutt, L.K., Pataer, A., Pahler, J., Fang, B., Roth, J., McConkey, D.J. and Swisher, S.G. (2002) *J. Biol. Chem.* 277, 9219–9225.
- [25] Nutt, L.K., Chandra, J., Pataer, A., Fang, B., Roth, J., Swisher, S.G., O'Neil, R.G. and McConkey, D.J. (2002) *J. Biol. Chem.* 277, 20301–20308.
- [26] Mehmet, H. (2000) *Nature* 403, 29–30.
- [27] Basanez, G., Nechushtan, A., Drozhinin, O., Chanturiya, A., Choe, E., Tutt, S., Wood, K.A., Hsu, Y., Zimmerberg, J. and Youle, R.J. (1999) *Proc. Natl. Acad. Sci. USA* 96, 5492–5497.